we obtained $\beta_1 = 1.0 \pm 0.5$ for the formation constant of $Eu(SCN)^{2+}$ in agreement with the results of solvent extraction[3] and UV spectroscopy. In the complex, the C–S stretching band is shifted to higher wavenumbers compared to free SCN^-. This behavior has been correlated with the coordination of SCN^- through the nitrogen.[28] When S is the donor atom, the C–S stretching is observed at lower wavenumbers.

IV. Conclusion

The NMR, UV, and Raman experiments reported in this work concur to show that the binding of thiocyanate ions to trivalent lanthanide ions gives rise to inner-sphere complexes. The NMR spectroscopy indicates in particular that the spin density delocalized from the metal ions to the directly bonded nitrogen atom of the SCN^- ligand is of the same order as that found for oxygen in the water solvation molecules.[17] A similar situation was found in the case of cobalt(II) aqueous thiocyanate complexes[29] except that the spin density transferred from Co(II) to nitrogen is of an order of magnitude higher than that reported here for Ln(III) SCN^- complexes.

The disagreement between the conclusions of this work and those of other authors[3-6] concerning the nature of lanthanide(III) thiocyanate complexes is possibly due to the difficulty to deduce this nature from the variation of thermodynamic constants. In the case of thiocyanato complexes, these constants are indeed very small ($\Delta H = 0.8$ kcal mol^{-1}, $\Delta S = 4.6$ cal deg^{-1} mol^{-1} [6]) and the experimental uncertainties are probably important as shown by the discrepancies between the values reported in different works.[3,6] Moreover, the variations of thermodynamic constants result from a large number of effects so that the semiempirical rules[30] relating the sign of these constants to the nature of the complexes are not necessarily valid in the case of the weak thiocyanate complexes.

Registry No. $[Pr(SCN)_2(H_2O)_7]^+$, 67905-00-4; $[Nd(SCN)_2(H_2O)_7]^+$, 67905-01-5; $[Eu(SCN)_2(H_2O)_7]^+$, 67905-02-6; $[Gd(SCN)_2(H_2O)_7]^+$, 67905-03-7; $[Tb(SCN)_2(H_2O)_7]^+$, 67905-04-8; $[Dy(SCN)_2(H_2O)_7]^+$, 67905-05-9; $[Ho(SCN)_2(H_2O)_7]^+$, 67905-06-0; $[Yb(SCN)_2(H_2O)_7]^+$, 67905-07-1; ^{13}C, 14762-74-4; SCN^-, 302-04-5.

References and Notes

(1) (a) C.E.N. de Fontenay-aux-Roses. (b) C.E.N. de Saclay.
(2) (a) J. P. Surls, Jr., and G. R. Choppin, *J. Inorg. Nucl. Chem.*, **4**, 62 (1957). (b) P. Th. Gerontopoulos, L. Rigali, and P. G. Barbano, *Radiochim. Acta*, **4**, 75 (1965).
(3) P. K. Khopkar and J. N. Mathur, *J. Inorg. Nucl. Chem.*, **36**, 3819 (1974).
(4) G. R. Choppin and J. Ketels, *J. Inorg. Nucl. Chem.*, **27**, 1335 (1965).
(5) H. D. Harmon, J. R. Peterson, J. T. Bell, and W. J. C. McDowell, *J. Inorg. Nucl. Chem.*, **34**, 1711 (1972).
(6) W. F. Kinard and G. R. Choppin, *J. Inorg. Nucl. Chem.*, **36**, 1131 (1974).
(7) N. Bloembergen, *J. Chem. Phys.*, **27**, 595 (1957).
(8) J. Reuben, G. H. Reed, and M. Cohn, *J. Chem. Phys.*, **52**, 161 (1970).
(9) N. Bloembergen, *J. Chem. Phys.*, **27**, 572 (1957).
(10) I. Solomon, *Phys. Rev.*, **99**, 559 (1955).
(11) R. Countryman and W. S. McDonald, *J. Inorg. Nucl. Chem.*, **33**, 2213 (1971).
(12) S. Koenig and M. Epstein, *J. Chem. Phys.*, **63**, 2279 (1975).
(13) T. J. Swift and R. E. Connick, *J. Chem. Phys.*, **37**, 307 (1962).
(14) A. D. McLachlan, *Proc. R. Soc. London, Ser. A*, **280**, 271 (1964).
(15) J. Reuben, *J. Phys. Chem.*, **75**, 3164 (1971).
(16) B. Bleaney, *J. Magn. Reson.*, **8**, 91 (1972).
(17) J. Reuben and D. Fiat, *J. Chem. Phys.*, **51**, 4909 (1969).
(18) F. Keffer, T. Oguchi, W. O'Sullivan, and J. Yamashita, *Phys. Rev.*, **115**, 1553 (1959).
(19) See for instance G. N. La Mar in "NMR of Paramagnetic Molecules", Academic Press, New York, N.Y., 1973, p 95.
(20) C. K. Jørgensen, *Mol. Phys.*, **5**, 271 (1962).
(21) J. C. Barnes, *J. Chem. Soc.*, 3880 (1964).
(22) J. C. Barnes and P. Day, *J. Chem. Soc.*, 3886 (1964).
(23) L. J. Nugent, R. D. Baybarz, J. L. Burnett, and J. L. Ryan, *J. Phys. Chem.*, **77**, 1528 (1973).
(24) S. Ahrland, *Acta Chem. Scand.*, **3**, 783 (1949).
(25) L. E. Orgel and R. S. Mulliken, *J. Am. Chem. Soc.*, **79**, 4839 (1957).
(26) H. Taube, *Prog. Stereochem.*, **3**, 121 (1962).
(27) J. L. Martin, L. C. Thompson, L. J. Radonovich, and M. D. Glick, *J. Am. Chem. Soc.*, **90**, 4493 (1968).
(28) R. A. Bailey, S. L. Kozok, T. W. Michelsen, and W. N. Wills, *Coord. Chem. Rev.*, **6**, 407 (1971).
(29) A. H. Zeltmann and L. O. Morgan, *Inorg. Chem.*, **9**, 2522 (1970).
(30) S. Ahrland, *Helv. Chim. Acta*, **50**, 306 (1967).

Contribution from the Departments of Chemistry, Southern Illinois University at Carbondale, Carbondale, Illinois, and University of Vermont, Burlington, Vermont 05401

Comparison of the Electrochemical Properties and Electron Spin Resonance Spectra of Thio and Imino Chelates

FRED C. SENFTLEBER and WILLIAM E. GEIGER, JR.*

Received July 7, 1978

Electrochemical reduction and oxidation of square-planar nickel, palladium, and platinum complexes of the bidentate ligand $(NH)_2C_2(CN)^{2-}$ have been accomplished. The general electron-transfer series $MN_4^+ \rightleftharpoons MN_4^0 \rightleftharpoons MN_4^- \rightleftharpoons MN_4^{2-}$ is detected, where N_4 stands for 2 mol of the ligand. Cyclic voltammetry and phase-selective ac polarography establish the electron-transfer steps as rapid and reversible. Visible and near-IR spectra of the anions are greatly similar to those observed previously for the corresponding MS_4^- complexes, in which sulfur replaces NH in the chelate structure. Electron spin resonance spectra of the anions show that the half-filled orbital is highly delocalized over the chelate structure, and metal hyperfine splittings suggest that, in PtN_4^-, the unpaired electron is more *ligand localized* than in PtS_4^-. An unequivocal determination of the electronic ground states of these complexes could not be made, but the ESR spectra are more consistent with the ^2A_g ground state than with the $^2B_{2g}$ ground state formed for the analogous dithiolate chelates.

Square-planar metal dithiolate complexes which undergo reversible electron-transfer reactions have been widely studied.[1] Syntheses of analogous chelates with other donor groups (e.g., O or NH) have been reported,[2-8] but characterization of the electron-transfer properties and electronic structures of these complexes has been less complete. Reductions of imino or oxo complexes are more difficult to achieve since these complexes have a lower electron affinity than the thio chelates[2-4] and at

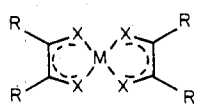

1, X = NH
2, X = S
3, X = O

* To whom correspondence should be addressed at the University of Vermont.

Table I. Voltammetric Data for MN_4 Complexes

compd	solvent	redox process	polarography			cyclic voltammetry	
			$E_{1/2}$[a]	slope[b]	i_a/i_c[c]	scan rate[d]	Δe_p[e]
NiN_4	glyme	$0 \rightleftarrows 1-$	−0.36	60.2	0.98	50	62
					0.96	500	63
		$1- \rightleftarrows 2-$	−1.18	60.3	0.97	50	60
					1.00	500	62
PdN_4	THF	$0 \rightleftarrows 1-$	−0.43	60.2	0.96	50	66
					0.92	500	66
		$1- \rightleftarrows 2-$	−1.08	61.9	1.07	50	62
					1.01	500	64
PtN_4	glyme	$0 \rightleftarrows 1-$	−0.52	60.3	0.97	50	59
					0.99	500	59
		$1- \rightleftarrows 2-$	−1.28	60.8	0.98	50	62
					1.01	500	62

[a] Volts vs. SCE. [b] Slope of plot of $-E$ vs. log $[i/(i_d - i)]$ in mV. [c] Ratio of anodic to cathodic peak currents. [d] mV/s. [e] Separation between cathodic and anodic peak currents in mV.

least some appear subject to slower electron-transfer processes.[9] The resultant difficulties in obtaining electron spin resonance (ESR) spectra of the paramagnetic monoanions derived from these species has hindered development of a quantitative description of the bonding in these chelates.

We now report electrochemical and spectroscopic studies of the reduction (and, to a lesser extent, oxidation) products of Ni, Pd, and Pt complexes formed utilizing the deprotonated form of the ligand diaminomaleonitrile, $(NH_2)_2C_2(CN)_2$. The complexes formed (**1**, R = CN) are square planar around the metal[5,10] and are congeners of the important maleonitriledithiolate (mnt) complexes (**2**, R = CN).[11,12] The redox properties, electonic ground states, and degree of metal–ligand delocalization of the imino and thiolato complexes are then compared. Hereafter, these complexes are referred to as MN_4 and MS_4, respectively.

Experimental Section

Preparations. NiN_4 was prepared by a modification of the method of Miles et al.[5] Use of anhydrous reagents allowed a substantial increase in yield (to about 30%). A nickel chloride–dimethoxyethane adduct was formed by refluxing anhydrous nickel chloride (2.5 mmol) in dry dimethoxyethane. After about 2 h, a yellow precipitate had formed. After the mixture was cooled to room temperature, 5.0 mmol of diaminomaleonitrile, dmn (Terramarine Bioresearch, recrystallized three times from ethyl acetate and vacuum dried), was added, and the solution was rendered basic by dropwise addition of 10.0 mmol of triethylamine. The intensely blue-green solution was filtered and evaporated, and the resulting powder was washed repeatedly with water. Final purification was accomplished using preparative-scale liquid chromatography employing a microstyragel column and tetrahydrofuran as the solvent. PdN_4[5] and PtN_4[10] were prepared by the literature methods. Again, preparative liquid chromatography was used for final purification. PdS_4^{2-} and PtS_4^{2-} were prepared as their tetra-*n*-butylammonium salts by published procedures.[13] The deuterated complex $Ni[(ND)_2C_2(CN)_2]_2$ was prepared by dissolving 20 mg of NiN_4-h_4 in 25 mL of acetone containing 4 mL of D_2O. After 24 h of stirring, the solution was filtered and evaporated. IR spectra of the product showed a strong N–D stretch (at ca. 2400 cm^{-1}) and only a low-intensity N–H stretch (ca. 3300 cm^{-1}). We estimate that about 90% deuteration was achieved. A ^{61}Ni-enriched NiN_4 sample was prepared using 11.5 mg of ^{61}Ni-enriched metal (90%, Oak Ridge). The nickel was dissolved in 1:1 nitric acid, heated to near dryness, and treated with a solution of 50 mg of dmn in 7 mL of methanol. After addition of a few drops of Me_3N, the solution turned deep green. After 1 h of stirring, the solution was evaporated and the residue washed several times with H_2O. The residue was dissolved in acetone, filtered, and evaporated to yield a small amount of $^{61}NiN_4$.

Solvents and Supporting Electrolytes. Acetonitrile and *N,N*-dimethylformamide (DMF) were both spectroquality (MCB). The former was stirred for 24 h over CaH_2, degassed, and stored under vacuum. The latter was dried several days over Linde type 4A molecular sieves, decanted, and vacuum distilled from *o*-phthalic acid. 1,2-Dimethoxyethane (glyme) and tetrahydrofuran (THF) were dried over either $LiAlH_4$ or Na, distilled, and stored under vacuum. Bu_4NPF_6 supporting electrolyte was prepared by mixing a slight excess of 65% HPF_6 with an alcoholic solution of Bu_4N (Southwestern Analytical Chemicals) and was recrystallized several times from 95% ethanol before vacuum drying. Electrolyte solutions were made 0.1 M in Bu_4NPF_6. Mercury was chemically purified by the method of Booth and Jones[14] before twice being distilled. All potentials are referred to the aqueous SCE.

Instrumentation. Princeton Applied Research Models 170 and 173 potentiostats were used for electrochemical experiments. Recording equipment, etc., was as previously described.[15] Most electrochemical experiments were done using a nitrogen purge to eliminate oxygen, but bulk coulometry experiments were performed using the vacuum electrochemical cells described elsewhere.[15] Electronic spectra of the ions were obtained by electrolytic reduction in a spectroelectrochemical cell which operated in the transmission mode. In these experiments a mercury pool cathode was aligned just below the optical light path in the spectrophotometer (Cary 14) and a solution was exhaustively electrolyzed at a potential appropriate for formation of the anion. ESR spectra was recorded with a Varian V-4502 spectrometer using a dual cavity with DPPH as a *g*-value standard. Paramagnetic MN_4 anions were prepared in one of two ways. In some cases, solutions of the anions produced by bulk electrolysis under nitrogen were syringed into ESR sample tubes. Typically, these samples were obtained after completion of coulometric experiments. Alternatively, solutions of MN_4 were electrolyzed in an intra muros cell[16] directly in the microwave sample cavity and quick-frozen if desired. Computer simulation of ESR spectra and other computations utilized a Xerox Sigma-6 computer.

Results

Electrochemistry. The reduction of the MN_4 complexes at mercury electrodes was investigated by dc and ac polarography, cyclic voltammetry, and controlled-potential coulometry. Each complex is reduced in two one-electron steps to MN_4^- and MN_4^{2-}.

Formation of MN_4^- and MN_4^{2-}. Figure 1 shows a dc polarogram of NiN_4 in dimethoxyethane. Two reduction waves of approximately equal height are accompanied by a small wave at about −0.7 V. This small wave is apparently due to adsorption of the complex and will be discussed later. The same pattern of waves was observed for all three complexes [NiN_4, PdN_4, PtN_4 (Table I)]. The two main waves were diffusion controlled, as shown by plots of limiting currents vs. square root of mercury column height which were linear and passed through the origin. Plots of dc potential vs. log $[i/(i_d - i)]$ gave slopes of −59 to −62 mV for both Faradaic waves of each complex. These values are consistent with each reduction being an electrochemically reversible one-electron transfer.

Phase-selective ac polarography confirmed both the electrochemical reversibility of the reductions and the adsorptive nature of the wave just negative of the first Faradaic process.

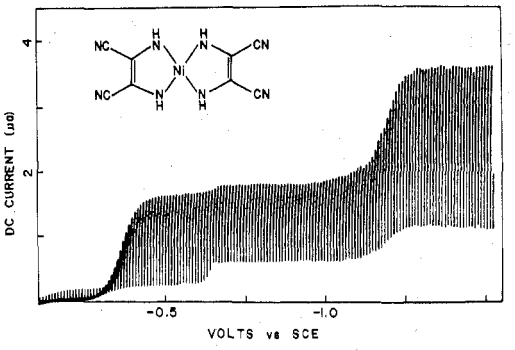

Figure 1. Dc polarogram of 3.0×10^{-4} M NiN_4 in 1,2-DME/Bu_4NPF_6 (1,2-DME = 1,2-dimethoxymethane).

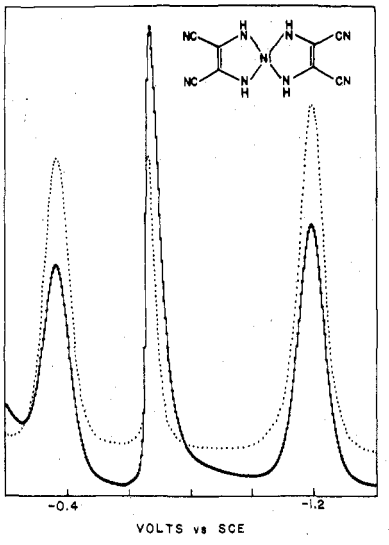

Figure 2. Ac polarogram of 4.3×10^{-4} NiN_4 in CH_3CN/Bu_4NPF_6 at 200 Hz: dotted line, in-phase component; solid line, out-of-phase component.

Figure 2 shows both the in-phase and out-of-phase components of an ac polarogram (at a frequency of 200 Hz) of NiN_4 in CH_3CN. The two symmetric peaks at −0.35 and −1.17 V correspond to the dc half-wave potentials of the two stepwise reductions to NiH_4^- and NiN_4^{2-}. From the observed currents, a standard rate constant for heterogeneous electron transfer, k_s, was calculated. The ratio of the in-phase to out-of-phase peak currents, cot ϕ, is related to k_s, D_0 (the diffusion coefficient of the oxidized form NiN_4), and ω (2π times the ac frequency) by eq 1.[17] The diffusion coefficient for NiN_4

$$\cot \phi = 1 + (2\omega D_0)^{1/2}/2k_s \qquad (1)$$

was measured from our dc polarographic data as $D_0 = 1.20 \times 10^{-5}$ cm^2/s. Ac measurements at frequencies of 50, 100, and 200 Hz gave average values of $k_s = 0.25 \pm 0.03$ and 0.29 ± 0.04 cm s^{-1} for the reductions $NiN_4^0 \rightleftarrows NiN_4^-$ and $NiN_4^- \rightleftarrows NiN_4^{2-}$, respectively. These values correspond to highly reversible electron transfers giving no evidence of important structural changes during the charge transfer. Hence it is likely that the anions and dianions retain the square-planar structure. The electron-transfer rates are only slightly lower than those reported for oxidation and reduction of MS_4^{2-}.[15,18,19] Thus, the reductions of these imino chelates are not subject to the slow electron transfers seen for some oxo chelates.[9,19]

The ac polarogram of NiN_4 (Figure 2) also shows the asymmetric peak at ca. −0.7 V, referred to previously, in which the out-of-phase (capacitive) component is considerably *greater* than the in-phase (resistive) component. This behavior is typical of adsorption-controlled processes[20a] and has been observed for other metal complexes.[20b] The ac polarograms

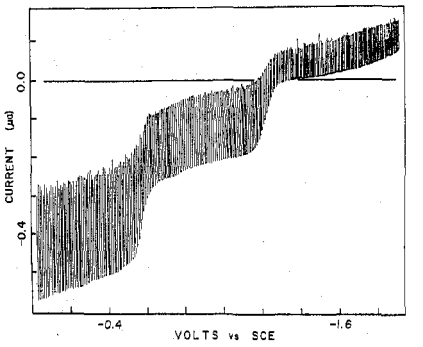

Figure 3. Dc polarogram of 2.5×10^{-4} M solution of PtN_4^{2-} made by electrolysis of PtN_4 at −1.6 V in 1,2-DME/Bu_4NPF_6.

of PdN_4 (in THF) were similar to those of the Ni complex, with Faradaic peaks at −0.43 and −1.08 V and an adsorption peak at −0.55 V. Adsorption problems were even more severe, however, for PdN_4, to the extent that the capacitive component to the ac wave was distorted in the region of the first reduction and k_s values could not be calculated for the PdN_4 reductions.

These complexes were also investigated by cyclic voltammetry (CV) at a hanging mercury drop electrode (HMDE). A variety of criteria established that the reductions were uncomplicated reversible charge transfers to give anions which were stable on the CV time scale (Table I). At slow scan rates, separations between the cathodic and anodic peaks were about 60 mV in agreement with value expected for a Nerstian system.[21] Cathodic current functions were constant as a function of scan rate, also consistent with a charge transfer uncomplicated by coupled chemical reactions.

The long-term stability of the anions, required for synthetic or spectroscopic investigations, was investigated by controlled-potential coulometry. These studies established that all of the anions except NiN_4^{2-} are indefinitely stable under strictly anaerobic conditions. Typical of these results is the behavior of PtN_4^{2-} in dimethoxyethane. The polarogram after electrolysis of PtN_4 at −1.6 V shows (Figure 3) two waves resulting from oxidation of the *dianion* of PtN_4. The heights of the anodic waves were equal to the heights of the cathodic waves of the original PtN_4 solution, showing that complete conversion to PtN_4^{2-} had been effected.

The number of electrons transferred (n) and the anion stabilities were further studied by reversal coulometry. In this approach the compound is initially reduced for a given length of time, t, and then reoxidized for the same amount of time. The number of electrons transferred in the reduction, n, is calculated from a plot of log i vs. t, by reference to eq 2, in

$$\log i = (-pt/2.30) + \log nFVC_0p \qquad (2)$$

which p is a constant (the mass-transfer coefficient), F is Faraday's constant, C_0 is the bulk concentration of the starting complex, and V is the solution volume. p is evaluated from the slope of the line, and n is calculated from the intercept.[22] When the reduction product is stable and not subject to follow-up reactions, the numbers of coulombs consumed in the reduction (Q_f) and oxidation (Q_b) are theoretically related[22] by eq 3. Representative values of t were 1000–2000 s.

$$Q_b/Q_f = 1 - \exp(-pt) \qquad (3)$$

The values of n and Q_b/Q_f for $NiN_4^{0/-}$ (electrolysis potentials of −1.0 and 0 V) were 0.91 e and 0.95, respectively. The coulomb ratio compared very nicely with the value (0.96) measured by electronic integration. These data again show that the reduction of NiN_4 proceeds by one electron to a stable anion. Similar data were also obtained for the first PtN_4 reduction [n = 1.01 e, Q_b/Q_f = 0.38 (theory, eq 3), 0.38 (measd)]. However, the same technique (potentials of −1.5

Table II. Optical Spectra of Metal Diaminomaleonitrile Complexes

complex	solvent	band position[a] (a_M)[b]
$Ni[(NH)_2C_2(CN)_2]_2$	dimethoxyethane	14 680 (4.1)
$Ni[(NH)_2C_2(CN)_2]_2^-$	dimethoxyethane	10 320 (4.1)
$Pd[(NH)_2C_2(CN)_2]_2$	tetrahydrofuran	14 500 (4.0)
$Pd[(NH)_2C_2(CN)_2]_2^-$	tetrahydrofuran	8 930 (3.9)
$Pt[(NH)_2C_2(CN)_2]_2$	dimethoxyethane	15 810 (4.0)
$Pt[(NH)C_2(CN)_2]_2^-$	dimethoxyethane	12 500 sh, 11 980 (3.4), 11 610 (3.4)
$Pt[(NH)C_2(CN)_2]_2^{2-}$		16 000–20 000, poorly resolved weak bands

[a] In cm^{-1}. [b] log of absorbancy coefficient.

and −1.0 V) established that the NiN_4 *dianion* is unstable [n = 1.20 e, $[Q_b/Q_f]$(measd) is less than one-tenth of theory]. Exhaustive electrolysis of PtN_4 solutions at the potential of the second wave (−1.6 V) established that the dianion of PtN_4 is stable (vide ante, Figure 3), but no coulometry was performed on the second reduction. The Pd complex was investigated in less detail but it did appear that PdN_4^- and PdN_4^{2-} were stable species, so *the only anion of the series which showed any sign of decomposition reactions was* NiN_4^{2-}. Polarograms of solutions of NiN_4 after electrolysis at the second wave had very poorly defined waves. Thus, the decomposition of NiN_4^{2-} was not a simple oxidative regeneration of NiN_4 or NiN_4^-. In contrast, air oxidation of solutions of all other anions resulted in quantitative recovery of the neutral MN_4 complex.

The oxidation of these complexes was briefly probed by voltammetry in acetonitrile at the rotating platinum electrode or by CV at a platinum bead. Oxidation waves were observed at $E_{1/2}$ potentials of +0.64 V (Ni), +0.43 V (Pd), and +0.98 V (Pt). The NiN_4 oxidation was irreversible except at high scan rates (>5 V/s). PtN_4^+ was considerably more stable but follow-up reactions were still evident from slow CV scans. The Pd oxidation product appeared to film the electrode, and data on it were unreliable. Although these experiments were only of a preliminary nature, it does appear that cation radicals could be generated from these complexes at lower temperatures or in less reactive solvents (unfortunately, the complexes are virtually insoluble in CH_2Cl_2, which is an excellent solvent for stabilizing oxidized compounds).

Optical Spectra of the Anions. Spectra of the neutral complexes and of the monoanions were recorded in the visible and near-infrared regions. Each neutral complex has an intense visible absorption band in the range 630–700 nm (Table II). When solutions of the complexes were electrolyzed at the potential of the first reduction in a spectroelectrochemical cell, spectra of the monoanions were recorded. Each of the monoanions has an intense band in the near-IR region (e.g., Figure 4). Attempts to obtain clean spectra of the dianions were not successful. Electrolysis of PtN_4 at the potential of the second reduction gave spectra of the dianion contaminated by the monoanion. However, poorly resolved weaker bands (log $a_M \sim 3$) in the region 500–600 nm were attributed to PtN_4^{2-}. Our attempts to obtain spectra of PdN_4^{2-} (by either electrolysis or alkali-metal reductions) were frustrated by poor conversion of PdN_4^- to PdN_4^{2-}.

The spectra of these complexes are very reminiscent of those of nickel-group dithiolenes. Absorptions of the neutral metal dithiolene complexes shift into the near-IR when the complexes are reduced to monoanions. These intense, low-energy transitions, which have been attributed to charge-transfer bands, are not seen in the spectra of the metal dithiolene

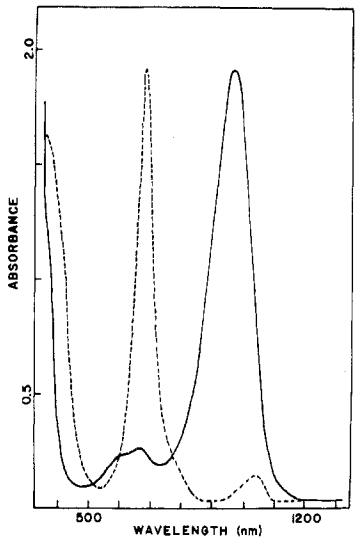

Figure 4. Visible–near-IR spectra of NiN_4 and NiN_4^- recorded using an in situ electrolysis cell: broken line, before electrolysis; solid line, after electrolysis at −0.80 V.

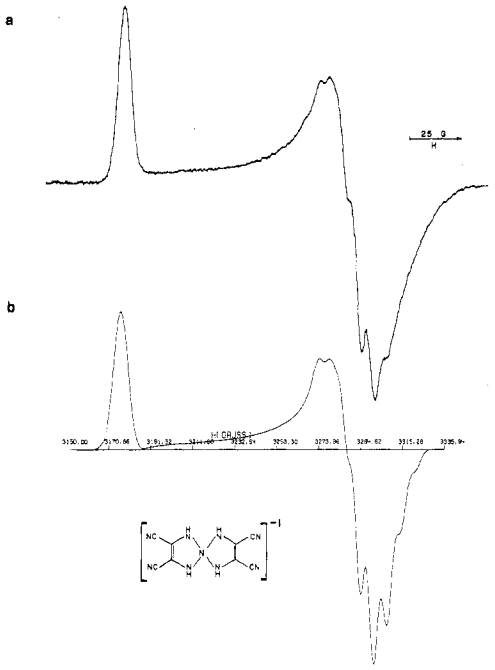

Figure 5. ESR spectra of NiN_4^- in a glass: (a) DMF/CH_3CN frozen-solution spectrum at 120 K; (b) computer-simulated spectrum using the parameters listed in Table III and line widths of 7 G for the low-field (g_1) feature and 6.3 G for the g_2 and g_3 components.

dianions. The similarity of the MN_4 and MS_4 spectra argues for qualitative similarities in the electronic structures of the two sets of complexes.

Electron Spin Resonance Spectra. As expected, the monoanions are paramagnetic. A solution containing electrogenerated NiN_4^- in a 2:1 DMF/CH_3CN solution gave a symmetric single-line ESR spectrum of 16-G peak-to-peak width. When this solution was frozen at 120 K, a spectrum of apparently axial symmetry resulted, with hyperfine splittings (hfs) visible on the $g_\perp$ component (Figure 5a). Since ^{61}Ni ($I = {}^3/_2$) has a very low natural abundance (1.2%), these splittings were ascribed to ^{14}N interactions arising from the ligands. Identical spectra were obtained in a 2-propanol glass (eliminating the possibility of CH_3CN or DMF coordination as the origin of the splittings) and for a sample in which the hydrogen atoms of the ligand were exchanged with deuterium.

Table III. ESR Parameters for Nickel-Group dmn and mnt Complexes

A. g Values

complex	medium	g_1	g_2	g_3	g_{iso}
NiN_4^-	DMF/CH_3CN	2.075	1.999	1.993	2.025
PdN_4^-	DMF/THF	2.062	2.004	1.958	2.008[a]
PtN_4^-	DMF/THF	2.225	1.983	1.843	2.020
NiS_4^-	crystal[b]	2.160	2.042	1.998	2.063
PdS_4^-	crystal[c]	2.071	2.043	1.956	2.024
PtS_4^-	crystal[d]	2.246	2.058	1.826	2.043

B. Hyperfine Splittings[e]

	$A_M(1)$	$A_M(2)$	$A_M(3)$	$A_M(iso)$	$A_N(1)$	$A_N(2)$	$A_N(3)$	$A_N(iso)$
NiN_4^-	22.9					5.4	6.5	
PdN_4^-	14.9					7.7		3.9[f]
PtN_4^-	107	195	154	156		7.9		
NiS_4^-[b]	14.9	3.0			4.6 (S)	4.6 (S)	14.3 (S)	
PdS_4^-[c]	10.3	5.9	5.4	7.4			16.8 (S)	
PtS_4^-[d]	8.1	128	100	78				

[a] Data taken in CH_3CN. [b] Data taken from ref 23 and 26. [c] Data taken from ref 25. [d] Data taken from ref 24. [e] Splittings in 10^{-4} cm^{-1}. [f] Calculated; see text.

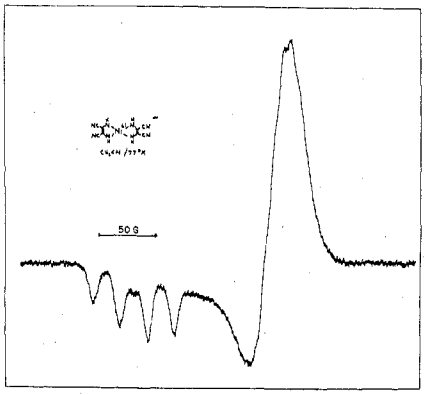

Figure 6. Frozen-solution ESR spectrum of NiN_4^- enriched 90% in ^{61}Ni. The ^{61}Ni hfs is clearly seen as a quartet along the g_1 feature.

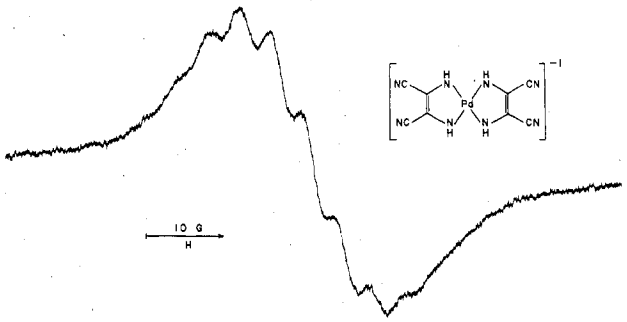

Figure 7. Fluid-solution ESR spectrum of PdN_4^- in CH_3CN/Bu_4NPF_6 at 300 K.

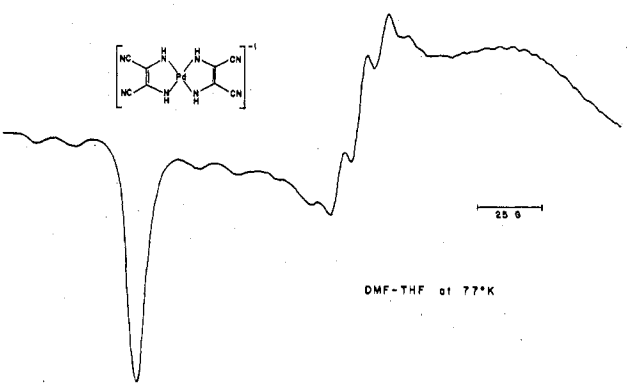

Figure 8. Frozen-solution ESR spectrum of PdN_4^- in DMF/THF at 77 K.

If the hfs were due to proton interactions, deuterium substitution would have led to a collapse of the hyperfine pattern since a ^2H splitting is about one-sixth of the ^1H splitting [g_N = 2.67 (^1H), 0.41(^2H)].

Extensive computer simulations of the $g_\perp$ region were performed in order to assign the splittings (Table III). The best fit (Figure 5b) was obtained with a slight deviation from axial symmetry in both the g value and the nitrogen hfs. Interaction with four equivalent nitrogens was calculated to be 5.8×10^{-4} and 7.0×10^{-4} cm^{-1} in the g_2 and g_3 components, respectively. Although the simulation shows better resolution than the experimental spectrum on the high-field side of the region, this probably arises from line-width effects resulting from broadening of the nitrogen lines arising from higher M_I values.

A frozen-solution spectrum of the Ni-61 enriched complex showed a well-resolved quartet along the $g_\parallel$ region arising from the Ni hfs (Figure 6). There was no apparent change in the $g_\perp$ region, meaning that the Ni splitting along $g_\perp$ is very small. A similar pattern has been observed for NiS_4^-.[23,24]

The isotropic spectrum of PdN_4^- was obtained from an acetonitrile solution of the anion transferred under nitrogen from the spectroelectrochemical cell to a quartz flat cell. Nitrogen hfs was clearly observed as nine lines due to interaction with four equivalent nitrogens ($a_N = 4.2 \times 10^{-4}$ cm^{-1}, Figure 7). No satellites due to Pd hfs (^{105}Pd, 22% abundant) were observed.

In a separate experiment, PdN_4^- was frozen at 77 K in a 2:1 DMF/THF solution and the glassy spectrum recorded (Figure 8). A rhombic **g** tensor is apparent, and, as with NiN_4^-, the largest metal splitting (14.9×10^{-4} cm^{-1}) is observed along the low-field component. This splitting was measured from the satellite lines around the low-field g component. Four of the six ^{105}Pd lines ($I = {}^5/_2$) are resolved, and their intensities were measured as 3.5% of the $I = 0$ line (theory = 4.7%). In the g_2 region, nitrogen hfs was seen (four equivalent N, nine lines, $a_N = 7.7 \times 10^{-4}$ cm^{-1}) but no metal splittings were observed. Along the high-field (g_3) direction, a complex hyperfine pattern was observed which we failed to decipher. However, using the assumptions that a_{N_1}(low field) = 0 and that all the N hfs are of the same sign, we can calculate that $a_{N_3} = 3.9 \times 10^{-4}$ cm^{-1}, using the measured values of a_{N_2} and a_{iso} and eq 4.

$$a_{iso} = {}^1/_3(a_1 + a_2 + a_3) \quad (4)$$

PtN_4^- was the only complex in which the metal hfs was observed for all three principal directions. Figure 9 shows the spectrum obtained from a frozen (77 K) DMF/THF solution

of the monoanion. All three central lines of the rhombic **g** tensor are flanked by a doublet arising from the ^{195}Pt splitting ($I = {}^1/_2$, 33.8% abundant). These satellites are all about the correct intensity (25.5%) compared to the unsplit parent line. A fluid-solution spectrum in CH_3CN allowed observation of the isotropic Pt splitting, which was quite large: 156×10^{-4} cm^{-1}. All of the Pt splittings have the same sign, as we can tell by comparing $a_{Pt}(iso)$ with the average of the three anisotropic splittings. If all three have the same sign, an average of 155×10^{-4} cm^{-1} is calculated, almost identical with the observed isotropic splitting. No well-resolved nitrogen hfs were observed for this complex, perhaps because the line widths were generally larger than in the other complexes. Splittings were observed along the middle g component which must be ascribed to nitrogen fine structure. These can be partially observed in Figure 9, but other spectra using long scan times and expanded magnetic field axes were used to make actual measurements. A nitrogen splitting of about 8×10^{-4} cm^{-1} seems to account for the splittings, but because of the poor resolution this number should not be taken too seriously.

Electronic Ground State Assignments

In using the ESR data to evaluate the nature of the half-filled orbital of the anions, we need to assign the molecular directions of the three principal **g** tensor components in the spectra. The following coordinate system is used:

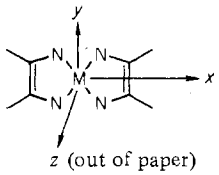

Since only the spectra of randomly oriented glasses of the ions could be produced, we assigned directions by analogy to previous single-crystal studies of MS_4^- and MSe_4^- complexes. Each of these studies showed that the g_1, g_2, and g_3 components (low to high field) were due to g_{yy}, g_{xx}, and g_{zz}, respectively,[23-27] and we assumed these directions in our data analysis.

Various ground states were considered for these complexes, using the general approach of Maki et al.[23] In this approach, the experimental observables (g values and metal hyperfine splittings) are related to the bonding parameters P and K through the configurational excitation energies C_i for each ground state. For example, equations for the $^2B_{2g}$ ground state, composed of a mixture of the metal d_{xz} orbital and ligand p_z orbitals, are given as eq 5–10.

$$g_{xx} = g_e + 2C_4 \quad (5)$$

$$g_{yy} = g_e - 6C_1 - 2C_3 \quad (6)$$

$$g_{zz} = g_e - 2C_2 \quad (7)$$

$$A_{xx} = P[2C_4 - K + {}^2/_7 + {}^3/_7(C_1 + C_2 - C_3)] \quad (8)$$

$$A_{yy} = P[-6C_1 - 2C_3 - K - {}^4/_7 - {}^3/_7(C_2 - C_4)] \quad (9)$$

$$A_{zz} = P[-2C_2 - K + {}^2/_7 + {}^3/_7(C_3 - C_1 - C_4)] \quad (10)$$

In these equations P and K are related to the anisotropic and isotropic parts, respectively, of the hyperfine tensor and are defined by eq 11 and 12. g_e is the free electron g value

$$P = g_e g_N \beta_e \beta_N \langle r^{-3} \rangle \quad (11)$$

$$K = [-{}^2/_3 \chi g_e g_N \beta_e \beta_N / hca_0^3]/p \quad (12)$$

(2.0023), g_N and β_N are the nuclear g value and nuclear magneton, respectively, and $\langle r^{-3} \rangle$ is the inverse cube electron–nucleus distance. χ is related to the spin polarization of s electrons by unpaired d electrons.[28,29] $C_1 = \xi/(E_{d_{z^2}} - E_{d_{xz}})$

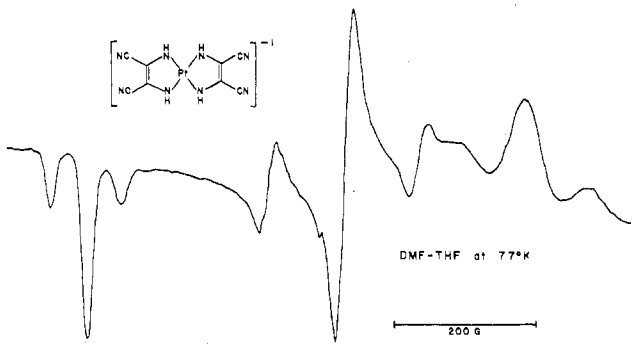

Figure 9. Frozen-solution ESR spectrum of PtN_4^- in DMF/THF at 77 K.

Table IV. Calculated Bonding Parameters for MN_4^- and MS_4^- Complexes for Various Possible Ground States

	NiN_4^-	NiS_4^-	PtN_4^-	PtS_4^- [d]
		$^2B_{2g}$		
K[a]	0.28	0.21	−1.49	−0.1
P[b]	29	24	107	270
P/P_0[c]	0.26	0.21	0.24	0.6
		^2A_g		
K	0.28	0.20	−1.29	−0.40
P	29	25	116	175
P/P_0	0.26	0.22	0.26	0.39

[a] Defined by eq 12 in text. [b] Defined by eq 11 in text; units of 10^{-4} cm^{-1}. [c] Value of $P_0 = 110 \times 10^{-4}$ cm^{-1} (Ni); 445×10^{-4} cm^{-1} (Pt). [d] Data taken from ref 24.

and the other constants involve excitation energies between the d_{xz} and d_{yz} (C_2), $d_{x^2-y^2}$ (C_3), and d_{xy} (C_4) orbitals.

In this treatment, P and K values are calculated for each possible ground state, based on the observed g and A values and a set of equations like (5)–(10) appropriate for that ground state [these equations are compiled in ref 23 (note that definition of the x and y directions are interchanged between our work and that of ref 23 and that the sign of C_4 in eq 15b of ref 23 has been shown[24] to be incorrect]. The sign and magnitude of P calculated for each ground state is then compared with the value (P_0) calculated for the free metal ion. The reasonableness of the K and P/P_0 values are then used to judge whether or not a particular ground state should be considered further as a possibility to describe the electronic structure of the complex. The ratio P/P_0 represents the lowering of the metal anisotropic parameter due to metal–ligand covalency and can be roughly taken as the degree of metal contribution in the half-filled orbital.

We also considered the possibility of an ^2A_g ground state configuration arising as a hybrid of the $d_{x^2-y^2}$ and d_{z^2} orbitals, which are allowed to mix in D_{2h} symmetry. This was not originally considered in the treatment of the metal dithiolenes but has since been discussed by Schlupp[24] and by McGarvey.[30] This orbital can be defined as $a(d_{z^2}) + b(d_{x^2-y^2})$ and would give rise to considerable *in-plane* anisotropy. Using the equations of Schlupp,[24] we calculated the values of $a^2 = 0.75$ and $b^2 = 0.25$ (for NiN_4^-) and $a^2 = 0.66$ and $b^2 = 0.34$ (for PtN_4^-) for this orbital.

The results of calculations of P and K for the two most probable ground states ($^2B_{2g}$ and ^2A_g) are given in Table IV. All other possible ground states gave unreasonable values for P/P_0 and/or K (e.g., a negative value of P/P_0). The results show that for either choice of ground state for MN_4^-, the metal only contributes about one-quarter to the half-filled orbital. Thus, both NiN_4^- and PtN_4^- have the unpaired electron delocalized throughout the chelate structure, just as does NiS_4^-. It does appear that PtN_4^- has considerably less metal character

to the unpaired electron than PtS_4^-. In this regard, the Pt hfs, which are considerably larger in the spectrum of PtN_4^-, are at first sight misleading, because their magnitude is due primarily to a large *isotropic* contribution. This is manifested in the large *negative* values of K calculated for PtN_4^- (Table IV). McGarvey has shown that K should be *positive* for third-row transition metals if the s character arises from spin polarization of the s electrons by the metal d electrons. A negative value such as we observe must be ascribed to *direct mixing* of the metal s orbital into the electronic ground state. Since this mixing must be rather large (3–4% contribution), the negative K value would seem to favor the ^2A_g ground state, which allows for direct mixing of the metal s and hybrid orbitals in D_{2h} symmetry.

However, the *ligand* (nitrogen) hfs hold the key to assignment of the ground state. McGarvey has pointed out that a measurable in-plane nitrogen hfs should accompany the ^2A_g ground state,[30] whereas the $^2B_{2g}$ ground state should give a large out-of-plane nitrogen splitting and small in-plane splittings. Indeed, Schmitt and Maki[26] used ^{33}S splittings to choose between the B_{2g} (d_{xz}) and A_g (d_{z^2}) ground states for NiS_4^-. They noted that the ^{33}S hyperfine tensor (A_{zz} = 14 × 10^{-4} cm^{-1}, $A_{xx} = A_{yy}$ = 4 × 10^{-4} cm^{-1}) was only consistent with the former (d_{xz}) description because the *unique* splitting was along the z (*high-field*) direction.

Assuming, as noted above, that g_1, g_2, and g_3 correspond to g_{yy}, g_{xx}, and g_{zz}, in our MN_4^- complexes the unique nitrogen hfs appears to be along the low-field (y) direction, and a measurable A_{xx} for nitrogen is seen along the g_2 direction.

This can be best seen in the spectrum of the Ni complex, which has a narrow low-field g_1 resonance. We estimated that splittings of as little as 2 G would be clearly visible on this component. On the other hand, much larger splittings (6–7 G) are observed in the x (g_2) and z (g_3) directions. Similarly, a large nitrogen splitting is observed for the x direction (g_2 component) for both PdN_4^- and PtN_4^-. By use of the arguments of Schmitt and Maki[26] and of McGarvey,[30] these observed ligand splittings cannot be reconciled with the $^2B_{2g}$ ground state. One further possibility which we considered was that the large a_N values along the g_{xx} direction arose from a misalignment of the principal directions of the ligand hyperfine tensor and the **g** tensor. This could still have allowed assignment of the $^2B_{2g}$ ground state. However, calculations reported in the Appendix show that coordinate misalignments cannot account for the magnitude of the apparent $a_N(x)$ splitting. We conclude that the ^2A_g ground state is the most likely description of the electronic structure of NiN_4^- and PtN_4^-.

It must be emphasized that this assignment cannot be unequivocal without confirmation that the **g** tensor directions are as assumed in the glassy spectrum. However, the high air sensitivity of the anions may preclude examinations of their single-crystal spectra.

As a final point, calculations may be carried out using the observed nitrogen splittings to estimate the nitrogen spin density. The s- and p-orbital spin densities on nitrogen can be calculated through eq 13–16.

$$A_{\parallel} = A_{iso} + 2B \quad (13)$$

$$A_{\perp} = A_{iso} - B \quad (14)$$

$$C_s^2 = A_{iso}/A_{calcd} \quad (15)$$

$$C_p^2 = B/B_{calcd} \quad (16)$$

Thus, the nitrogen spin densities C_s^2 and C_p^2 are obtained by comparison of the isotropic and anisotropic parts of the nitrogen hyperfine tensor (A_{iso} and B, respectively) with the calculated versions of those quantities which assume complete localization of the unpaired electron in either the s or p orbital.

Table V

A_{xx}, G	A_{yy}, G	θ, deg
5.80	1.99	2.0
5.85	1.86	8.0
6.05	1.09	17.0
6.46	−1.89	25.0

Values of A_{calcd} and B_{calcd} depend on the values of $|\chi_{2s}(0)|^2$ and $\langle r^{-3}\rangle_{2p}$ chosen for nitrogen. We used the values calculated by Morton et al.,[31] in which A_{calcd} = 552 G and B_{calcd} = 17.2 G. Coupled with our experimental values of A_{iso} = 4.3 G and B = 2.1 G, these equations yield C_s^2 = 0.008 and C_p^2 = 0.12. In order to carry out these calculations, we assumed that the unresolved $A(y)$ splitting was zero and that all the nitrogen splittings were of the same sign. These results place half of the unpaired spin directly on the four coordinating nitrogens and confirm that the bulk of the unpaired spin is on the ligand.

Comparison of MN_4 and MS_4

In their overall properties, the imino and thio chelates are rather similar. Each set of complexes can exist (albeit sometimes transiently) in four of the five states of the general electron-transfer series

$$MX_4^+ \rightleftharpoons MX_4 \rightleftharpoons MX_4^- \rightleftharpoons MX_4^{2-} \rightleftharpoons MX_4^{3-}$$

The main difference in electrochemical behavior stems from the lower electron affinity of the nitrogen complexes. Standard reduction potentials are about 1.5 V more positive for the MS_4 complexes.[32] This makes the $MN_4^{2-/3-}$ couple electrochemically inaccessible because of the limited cathodic window (to −2.8 V) of our electrolytes. Conversely, it is the most oxidized form, MS_4^+, which remains undetected for these MS_4 complexes with strong electron-withdrawing (cyano) substituents. Each set of complexes gives rapid, reversible electron transfers in nonaqueous media. The electronic distributions (metal vs. ligand) are qualitatively similar and result in close analogies in electronic spectra and in potential separations between successive redox steps.[32] It does appear that there is higher localization on the metal in PtS_4^- than in PtN_4^-. Finally, there is sufficient evidence in favor of the ^2A_g ground state for MN_4^- that it should be given strong consideration in discussions of these complexes.

Acknowledgment. The authors are grateful to the National Science Foundation for the support of this work and are indebted to A. H. Maki for providing access to data prior to publication and to Professor Maki, R. L. Schlupp, and R. D. Bereman for helpful discussions.

Appendix

Consideration of Possible Misalignment of Principal Directions of Nitrogen Hyperfine Tensor and g Tensor. This could result in an unexpectedly high value of $a_N(2)$ because the g_2 direction would not lie along a minimum in the nitrogen hfs. Such an effect has been observed in the ESR spectrum of a related complex, $Ni[Se_2C_2(CF_3)_2]_2^-$.[24] In this situation, there are a family of solutions to the ligand hyperfine tensor which reproduce the observed hfs.[33] The solutions involve the A_{xx} and A_{yy} hyperfine components and the angle of noncoincidence, θ, of the in-plane ligand hfs and **g** value tensors.

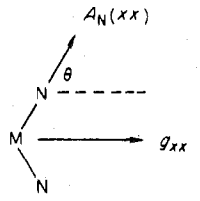

In principle, one can choose the correct solution from the set of possible solutions because each solution predicts small

differences in the spacing of the ligand hyperfine lines, and these predictions can be mated with experimental observations. This approach yielded a value of $\theta = 32-36°$ for the nickel–selenium complex mentioned above.[24]

Since our ligand hfs was not sufficiently resolved to allow observation of small deviations from the normally equal spacing of the hyperfine components, we sought to answer only one question with this technique: was there *any* reasonable value of θ which would allow a very small value of A_{xx} to be consistent with the observed nitrogen splitting along the g_{xx} direction? An answer of *no* would mean that the d_{xz} ground state could be eliminated from consideration. Table V gives a representative sampling of the values of A_{yy}, A_{xx}, and θ which reproduce the observed values of $A_1(N)$ and $A_2(N)$. These results showed that (for calculations up to $\theta = 40°$) the observed $A_2(N)$ splitting of 5.8 G was the *minimum* value possible for $A_{xx}(N)$. This fact argues against the $^2B_{2g}$ ground state for NiN_4^-, and, by implication, PtN_4^-, which also has a large splitting for $A_2(N)$.

Registry No. NiN_4, 34303-07-6; PdN_4, 34303-08-7; PtN_4, 34341-53-2; NiN_4^-, 67904-96-5; PdN_4^-, 67904-97-6; PtN_4^-, 67904-98-7; PtN_4^{2-}, 67904-99-8.

References and Notes

(1) This subject has been extensively reviewed: (a) J. A. McCleverty, *Prog. Inorg. Chem.*, **10**, 49 (1968); (b) G. N. Schrauzer, *Transition Met. Chem.*, **4**, 299 (1968); (c) G. N. Schrauzer, *Acc. Chem. Res.*, **2**, 72 (1969); (d) J. A. McCleverty in "Reactions of Molecules at Electrodes", N. S. Hush, Ed., Wiley-Interscience, New York, N.Y., 1971, p 403.
(2) A. L. Balch, F. Rohrscheid, and R. H. Holm, *J. Am. Chem. Soc.*, **87**, 2301 (1965).
(3) A. L. Balch and R. H. Holm, *J. Am. Chem. Soc.*, **88**, 5201 (1966).
(4) T. R. Miller and I. G. Dance, *J. Am. Chem. Soc.*, **95**, 6970 (1973).
(5) M. G. Miles, M. B. Hursthouse, and A. G. Robinson, *J. Inorg. Nucl. Chem.*, **33**, 2015 (1971).
(6) F. Rohrscheid, A. L. Balch, and R. H. Holm, *Inorg. Chem.*, **5**, 1542 (1966).
(7) A. L. Balch, *J. Am. Chem. Soc.*, **91**, 1948 (1969).
(8) L. F. Warren, *Inorg. Chem.*, **16**, 2814 (1977).
(9) A. M. Bond, R. L. Martin, and A. F. Masters, *Inorg. Chem.*, **14**, 1432 (1975).
(10) J. W. Lauher and J. A. Ibers, *Inorg. Chem.*, **14**, 640 (1975).
(11) H. B. Gray, R. Williams, I. Bernal, and E. Billig, *J. Am. Chem. Soc.*, **84**, 3596 (1962).
(12) A. Davison, N. Edelstein, R. H. Holm, and A. H. Maki, *J. Am. Chem. Soc.*, **85**, 2029 (1963).
(13) A. Davison and R. H. Holm, *Inorg. Synth.*, **10**, 19 (1967).
(14) H. S. Booth and N. C. Jones, *J. Ind. Eng. Chem.*, **19**, 104 (1927).
(15) W. E. Geiger, Jr., T. E. Mines, and F. C. Senftleber, *Inorg. Chem.*, **14**, 2141 (1975).
(16) A. H. Maki and D. H. Geske, *J. Chem. Phys.*, **30**, 1356 (1959).
(17) D. E. Smith, *Electroanal. Chem.*, **1**, 1 (1966).
(18) P. J. Lingane, *Inorg. Chem.*, **9**, 1162 (1970).
(19) A. M. Bond, R. L. Martin, and A. F. Masters, *J. Electroanal. Chem.*, **72**, 187 (1976).
(20) (a) M. Sluyters-Rehbach and J. H. Sluyters, *J. Electroanal. Chem.*, **65**, 831 (1975); (b) M. C. Hughes and D. J. Macero, *Inorg. Chim. Acta*, **4**, 327 (1970).
(21) R. S. Nicholson, *Anal. Chem.*, **37**, 1351 (1965).
(22) K. S. V. Santhanam and A. J. Bard, *Electroanal. Chem.*, **4**, 215 (1970).
(23) A. H. Maki, N. Edelstein, A. Davison, and R. H. Holm, *J. Am. Chem. Soc.*, **86**, 4580 (1964).
(24) R. L. Shlupp, Ph.D. Thesis, University of California at Riverside, 1973.
(25) R. Kirmse and W. Dietzsch, *J. Inorg. Nucl. Chem.*, **38**, 255 (1976).
(26) R. D. Schmitt and A. H. Maki, *J. Am. Chem. Soc.*, **90**, 2288 (1968).
(27) R. Kirmse, W. Dietzsch, and B. V. Solovev, *J. Inorg. Nucl. Chem.*, **39**, 1157 (1977).
(28) A. Abraam, J. Horowitz, and M. H. L. Pryce, *Proc. R. Soc. London, Ser. A*, **230**, 169 (1955).
(29) B. R. McGarvey, *J. Phys. Chem.*, **71**, 51 (1967).
(30) B. R. McGarvey, *Can. J. Chem.*, **53**, 2498 (1975).
(31) J. R. Morton, J. R. Rowlands, and D. H. Whiffen, *Natl. Phys. Lab. Bull.*, **No. BPR 13** (1962).
(32) F. C. Senftleber and W. E. Geiger, Jr., *J. Am. Chem. Soc.*, **97**, 5018 (1975).
(33) Reference 23 gives a complete description of the equations used in these calculations. A computer program to accomplish the calculations is available either from the present authors or in ref 34.
(34) F. C. Senftleber, Ph.D. Thesis, Southern Illinois Univeristy, Carbondale, Illinois, 1977.

Contribution from the Christopher Ingold Laboratories, University College, London WC1H OAJ, England

Electronic Spectra and Resonance Raman Spectra of Mixed-Valence Linear-Chain Complexes of Platinum with 1,2-Diaminoethane

JEREMY R. CAMPBELL, ROBIN J. H. CLARK,* and PHILIP C. TURTLE

Received July 13, 1978

The resonance Raman spectra of the mixed-valence complexes $[Pt(en)X_2][Pt(en)X_4]$ and $[Pt(en)_2][Pt(en)_2X_2](ClO_4)_4$, en = 1,2-diaminoethane and X = Cl or Br, have been recorded at room temperature and at ca. 80 K by use of an excitation line whose wavenumber falls within the contours of the intense, axially polarized, mixed-valence bands of these complexes in the visible region. The resonance Raman spectra are characterized by the appearance of an intense progression $\nu_1\nu_1$, where ν_1 is the symmetric $X-Pt^{IV}-X$ stretching mode of the platinum(IV) moiety. This progression reaches $\nu_1 = 14$, 11, 14, and 10 for the above four complexes, respectively. Weak subsidiary progressions $\nu_n + \nu_1\nu_1$ also appear in the spectra, where ν_n (the enabling mode) is another Raman-active mode. From the observed progressions, the spectroscopic constants ω_1 and x_{11} are calculated for each complex. The excitation profile of the ν_1 band of all four complexes reaches a maximum near the band maximum of the axially polarized mixed-valence band of each complex, although in the case of $[Pt(en)Br_2][Pt(en)Br_4]$ another maximum in the excitation profile probably occurs near 13 000 cm^{-1}. The results suggest the use of the resonance Raman technique to detect and to resolve overlapped electronic absorption bands.

Introduction

Recent resonance Raman (RR) spectroscopic studies on mixed-valence complexes have focused on the linear-chain halogen-bridged variety, viz., $[Pt(etn)_4][Pt(etn)_4X_2]X_4 \cdot nH_2O$, etn = ethylamine, $n = 4$ (X = Cl or Br) and $n = 0$ (X = Br or I),[1-3] and $[trans\text{-}M(NH_3)_2X_2][trans\text{-}M'(NH_3)_2X_4]$, where M or M' = Pt or Pd and X = Cl or Br.[4,5] The present paper develops this subject further with a detailed study of the mixed-valence complexes $[Pt(en)X_2][Pt(en)X_4]$ and $[Pt(en)_2][Pt(en)_2X_2](ClO_4)_4$, where en = 1,2-diaminoethane and X = Cl or Br. The object of the investigation is to establish the nature of the resonance Raman spectra obtained when these complexes are excited with radiation which falls within the contour of the lowest energy mixed-valence transition in each case and, thus, to provide important spectroscopic information on the complexes. The neutral ones are known to possess the linear-chain halogen-bridged structure shown in Figure 1,[6] the $Pt^{II}-Pt^{IV}$ distance increasing in the order chloride

0020-1669/78/1317-3622$01.00/0